Variable-frequency EPR study of Mn²⁺-doped NH₄Cl₀.₉I₀.₁ single crystal at 9.6, 36, and 249.9 GHz: structural phase transition

Sushil K. Misra,[a,*] Serguei I. Andronenko,[a] Gino Rinaldi,[a] Prem Chand,[b]
Keith A. Earle,[c] and Jack H. Freed[c]

[a] *Physics Department, Concordia University, Montreal, Que., Canada H3G 1M8*
[b] *Physics Department, Indian Institute of Technology, Kanpur, UP 208016, India*
[c] *Baker laboratory, Department of Chemistry and Chemical Biology, Cornell University, Ithaca, NY 14853-1301, USA*

Received 27 June 2002; revised 1 November 2002

Abstract

Multifrequency electron paramagnetic resonance studies on the Mn²⁺ impurity ion in a mixed single crystal NH₄Cl₀.₉I₀.₁ were carried out at 9.62 (X-band) in the range 120–295 K, at 35.87 (Q-band) at 77 and 295 K, and at 249.9 GHz (far-infrared band) at 253 K. The high-field EPR spectra at 249.9 GHz are well into the high-field limit leading to a considerable simplification of the spectra and their interpretation. Three magnetically inequivalent, but physically equivalent, Mn²⁺ ions with their respective magnetic Z-axes oriented along the crystallographic [1 0 0], [0 1 0], [0 0 1] axes were observed. Simultaneous fitting of EPR line positions observed at X-, Q-, and far infra-red bands was performed using a least-squares procedure and matrix diagonalization to estimate accurately the Mn²⁺ spin-Hamiltonian parameters. The temperature variation of the linewidth and peak-to-peak intensities of the EPR lines indicate the presence of λ-transitions in the mixed NH₄Cl₀.₉I₀.₁ crystal at 242 and 228 K consistent with those observed in the pure NH₄Cl and NH₄I crystals, respectively. A superposition-model analysis of the spin-Hamiltonian parameters reveals that the local environment of the Mn²⁺ ion is considerably reorganized to produce axially symmetric crystal fields about the respective Z-axes of the three magnetically inequivalent ions as a consequence of the vacancy created due to charge-compensation when the divalent Mn²⁺ ion substitutes for a monovalent NH₄⁺ ion in the NH₄Cl₀.₉I₀.₁ crystal. This reorganization is almost the same as that observed in NH₄Cl and NH₄I single crystals, although the latter two are characterized by different, simple cubic and face-centered cubic, structures.

1. Introduction

Ammonium halides, which possess cubic crystal structures, are attractive materials for studying a variety of different structural phase transitions associated with ferroelectric or antiferroelectric ordering of the ammonium ions. The ferroelectric behavior of the mixed bromide–chloride NH₄Cl₁₋ₓBrₓ compounds was observed to differ from that of either the pure NH₄Cl and NH₄Br compounds [1]. Electron paramagnetic resonance (EPR) studies of heterovalent transition metal ions doped in alkali and ammonium halides are interesting because they provide an opportunity to study various sites available for occupation by impurity paramagnetic ions in the host materials, associated charge-compensating mechanisms, and the resulting environment in the vicinity of the probe impurity EPR ion. The EPR of Mn²⁺-doped NH₄Cl has been reported by several groups [2–11]. The nature of the site occupied by the Mn²⁺ ion has been controversial. Abe and Shirai [2] first reported values of the parameters D, A, and g from their EPR investigations of the Mn²⁺ ion in NH₄Cl crystal. Zaripov and Chirkin [3,4] obtained more precise values of these parameters from their temperature-dependent EPR investigations at 37 and 55 GHz, and determined the negative sign of the parameter D from their low-temperature experiment. X-band EPR studies of Forman and van Wyk on Mn²⁺-doped NH₄Cl [5,6] led to the observation of a complex EPR spectrum, due to the microwave quantum (X-band, 9.5 GHz) used

* Corresponding author. Fax: 1-514-848-2828.
   E-mail address: skmisra@vax2.concordia.ca (S.K. Misra).

being very close to one of the two electronic zero-field splittings (ZFS ~9 GHz). They concluded that when the divalent Mn^{2+} ion replaces the monovalent NH_4^+ ion in NH_4Cl, charge-compensation occurs by creation of a vacancy at the nearest-neighbor cation position in the vicinity of the manganese ion. Seed [7] suggested a different charge-compensation configuration from his study of Mn^{2+} EPR spectra, in which the Mn^{2+} ion was situated interstitially between two H_2O molecules on the boundary of two unit cells, substituting for an NH_4^+ ion. The appearance of numerous forbidden hyperfine EPR lines at X-band was investigated in detail by Lupei et al. [8]. Bramley and Strach [9] reported improved values of Mn^{2+} EPR parameters in NH_4Cl. Kennewell et al. [10] found only a small change in the value of the D parameter and no marked anomaly in the A parameter for the Mn^{2+} ion upon passing through the transition temperature near the λ-transition ($T_\lambda = 242$ K) in an NH_4Cl crystal. Van Wyk [11] found a small peak in the EPR linewidth near T_λ.

EPR spectra of the Mn^{2+} ion in NH_4I single crystal were first investigated by Chand et al. [12–14] at X- and Q-bands. Later, the temperature dependence of the EPR spectrum of the Mn^{2+} ion through two phase transitions, at 256 and 231 K, in NH_4I was reported by Chand [15], who found pronounced changes in the EPR spectrum, increasing EPR linewidth and decreasing peak-to-peak intensity near 256 K, as well as a much weaker effect at 231 K.

Alternative charge-compensation models [4,7,10] in Mn^{2+}-doped alkali halides crystals grown from aqueous solutions have also been proposed. In this model, the Mn^{2+} ion is associated with H_2O impurity molecules, which occupy the two nearest NH_4^+ positions on the same cubic axis. However, it was pointed out that this model was not valid [13,15] because heat treatment could easily affect EPR spectra in this case, concluding that charge-compensation occurs due to a vacancy in nearest-neighbor cation positions.

The Mn^{2+} ion doped in ammonium halide single crystals, e.g., NH_4Cl, NH_4I, is characterized by unusually large zero-field splittings (ZFS) for inorganic crystals [16] ($b_2^0 = D = -4.498$ GHz and -4.515 GHz for NH_4Cl and NH_4I, respectively, at room temperature) resulting in complex EPR spectra at X-band due to the microwave frequency not being sufficiently large compared to the ZFS. On the other hand, in the NH_4Br crystal in the tetragonal phase, Sastry [17] observed the Mn^{2+} D value to be quite small (~1.51 GHz) compared to that in NH_4Cl, and concluded that in this crystal Mn^{2+} enters substitutionally for NH_4^+ with the charge-compensating vacancy being far removed from the Mn^{2+} ion.

EPR at high frequencies can lead to a considerable simplification of spectra with a large ZFS. In favorable cases the value of D can be directly estimated from the

spectrum [18,19]. This greatly simplifies the spectral analysis. It is the purpose of this paper to report a multifrequency EPR study of the mixed crystal $NH_4Cl_{0.9}I_{0.1}$ doped with Mn^{2+}. Since the Cl^- and I^- ions possess different electronegativities, as well as different nuclear spins, their interactions may modify spin-Hamiltonian parameters in the mixed crystal $NH_4Cl_{0.9}I_{0.1}$ from those in the pure crystals. Further, both NH_4Cl and NH_4I single crystals exhibit structural phase transitions with decreasing temperature, from the $Fm3m$ space symmetry group to the $Pm3m$ space symmetry group, at 457 and at 256 K, respectively, as well as λ-transitions, at 242 and 231 K, respectively. Therefore, the mixed $NH_4Cl_{0.9}I_{0.1}$ crystal is also expected to exhibit similar structural phase transitions in this temperature range, which may be detected by EPR. The frequencies used in the study presented here are X-band (9.6 GHz), Q-band (35.87 GHz), and far-infrared (FIR) band (249.9 GHz). A multifrequency approach, fitting all EPR line positions observed at various frequencies simultaneously, enables one to estimate the SHP more precisely: the g values and ZFS parameters are determined more accurately at higher frequencies, while the hyperfine-structure (HF) parameters are determined more accurately at low frequencies [16,18].

2. Crystal growth and structure

Single crystals of the mixed compound $NH_4Cl_{0.9}I_{0.1}$ doped with Mn^{2+} were grown by slow evaporation of a stoichiometrically saturated aqueous solution to which ~0.1 wt% $MnCl_2$ was added. To prevent dendritic growth, ~2 wt% urea was added as growth modifier. The crystals were grown in the dark at 300 K to avoid photo-dissociation of ammonium iodide. Beautiful colorless cubic-shaped crystals of optical quality were obtained. The composition was verified by chemical analysis, while the single-crystal quality was checked by X-rays. The crystals possessed the SC (simple cubic: CsCl structure) of pure NH_4Cl at 300 K, and were characterized by perfect {1 0 0} cleavage planes.

The space group of NH_4Cl and NH_4I are O_h^1 ($Pm3m$) and O_h^5 ($Fm3m$) below and above their respective transition temperature (T_c); for NH_4Cl (CsCl: SC structure) $T_c = 457$ K [20] and for NH_4I (NaCl: FCC structure) $T_c = 256$ K [21]. The point group at the site of NH_4^+ ions is O_h for both crystals. NH_4Cl and NH_4I crystals undergo λ-transition from cubic O_h^1 (CsCl structure) to tetragonal D_{4h}^7 space group (PH_4I structure) at 242 and 231 K, respectively. Since NH_4Cl and NH_4I crystals possess different cubic structures, there are several sites available for substitution of the I^- ion in the NH_4Cl lattice, as well as different configurations for the charge-compensation states in the resulting mixed compound $NH_4Cl_{0.9}I_{0.1}$. The SC cubic structure with the positions

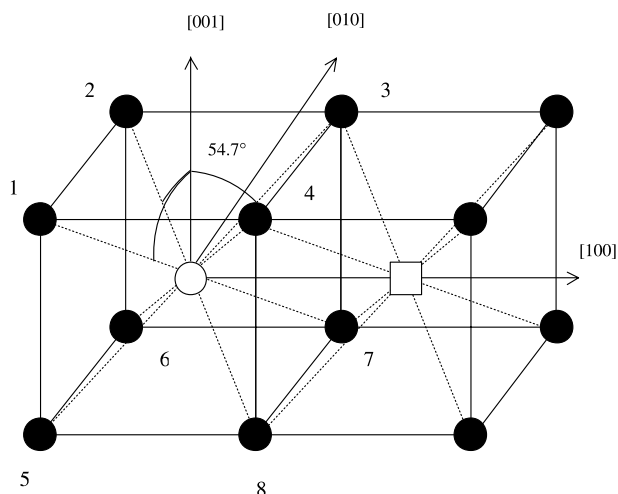Fig. 1. The structure of the $NH_4Cl_{0.9}I_{0.1}$ single crystal, showing the impurity ion Mn^{2+}, and the vacancy created due to charge-compensation and the ligand halide ions. Open circles are the cations NH_4^+, substituted for by the Mn^{2+} ion; black circles are the anions Cl^- or I^-; and square indicates a vacancy for charge-compensation. Similar vacancies are expected adjacent to the Mn^{2+} ion in the $[1\,0\,0]$, $[\bar{1}\,0\,0]$, $[0\,1\,0]$, $[0\,\bar{1}\,0]$, $[0\,0\,1]$, $[0\,0\,\bar{1}]$ directions.

of the various ions and possible vacancy site for charge-compensation due to substitution of a divalent Mn^{2+} ion at the site of a monovalent NH_4^+ ion in NH_4Cl is shown in Fig. 1.

3. EPR spectra and their interpretation: phase transition and spin-Hamiltonian parameters (SHP)

3.1. Experimental arrangement

EPR measurements at 249.9 GHz were carried out at 253 K at Cornell University on a spectrometer that uses a transmission Fabry–Pérot cavity in the warm bore of a superconducting magnet dewar with an ambient temperature of 253 K. The magnetic field can be varied from 0.0 to 9.3 T, the field modulation being 0.1–0.5 mT at approximately 100 kHz. General experimental details of the 249.9-GHz spectrometer can be found in [22]. In particular, the use of an In-Sb hot electron bolometer improved the S/N ratio by a factor of 5–10 [18]. The X- and Q-band measurements were made on Bruker and Varian spectrometers, respectively, at Concordia University; the former was equipped with an Bruker liquid-nitrogen accessory for temperature variation in the range 120–295 K, while the latter used a liquid nitrogen dewar for measurements at 77 K. The magnetic field was limited to 1.3 T at Q-band. The X-band measurements were carried out at room (295 K), liquid nitrogen (125 K), and in the temperature range 120–300 K, while those at Q-band were done at 295 and 77 K.

3.2. EPR spectra

The Mn^{2+} EPR spectra in the $NH_4Cl_{0.9}I_{0.1}$ single crystal at 9.62 GHz (295 K), 35.87 GHz (295 K), and 249.9 GHz (253 K) are exhibited in Fig. 2 for rotation of the external magnetic field **B** in the plane perpendicular to a cubic edge of the crystal. The VHF (249.9 GHz) spectra readily indicate the presence of three magnetically inequivalent, but physically equivalent, Mn^{2+} ions in the crystal with the respective magnetic Z-axes being oriented along the crystallographic axes, $[1\,0\,0]$, $[0\,1\,0]$, $[0\,0\,1]$. Thus, the Z-axis of one ion and the X- and Y-axes of the two other ions are found to be coincident. Furthermore, the EPR spectra for each of the three magnetically inequivalent Mn^{2+} ions about its magnetic Z-axis showed axial symmetry, so that the spectra for $B||X$ and Y-axes are the same. Each fine-structure (FS) line splits into six hyperfine (HF) lines as the ^{55}Mn nucleus (100% natural abundance) possesses nuclear spin $I = 5/2$ ($g_n = 1.382$). As seen from Fig. 2 it is relatively difficult to identify the lines belonging to the three magnetically inequivalent ions at X- and Q-bands. The angular variations of Mn^{2+} spectra were also recorded at lower temperatures: at 77 K (36.06 GHz) and at 125 K (9.69 GHz).

3.3. Temperature variation of EPR spectrum: phase transition

The temperature variation of the X-band EPR spectrum is expected to show changes in the Mn^{2+} EPR spectrum in $NH_4Cl_{0.9}I_{0.1}$ crystal, which are expected to be consistent with the λ-transitions at 241 and 231 K occurring, respectively, in the pure NH_4Cl and NH_4I crystals. The behavior of the widths and peak-to-peak intensities of the Mn^{2+} EPR hyperfine lines in the highest-field sextet for intermediate orientations of the external magnetic field, as shown in Fig. 3, clearly demonstartes the occurrence of the corresponding λ-transitions in the mixed crystal $NH_4Cl_{0.9}I_{0.1}$ at 245 ± 2 and 228–232 K. The transition at 228–232 K has a significantly weaker effect on the spectrum than that at 245 K and is spread out over an interval of 4 K, as indicated by the intensity and width of lines, presumably because of the much lower concentration of I^- ions (10%) as compared to that of Cl^- ions (90%) in the $NH_4Cl_{0.9}I_{0.1}$ crystal. Changes in the peak-to-peak intensity in the range 228–232 K occurred for other orientations of the magnetic field **B** as well.

3.4. Spin-Hamiltonian parameters (SHP)

The three magnetically inequivalent, but physically equivalent, ions are described by the same set of SHP. The EPR line positions for a magnetically inequivalent Mn^{2+} ion were fitted to the spin Hamiltonian (SH) appropriate to axial site symmetry [19,23]:
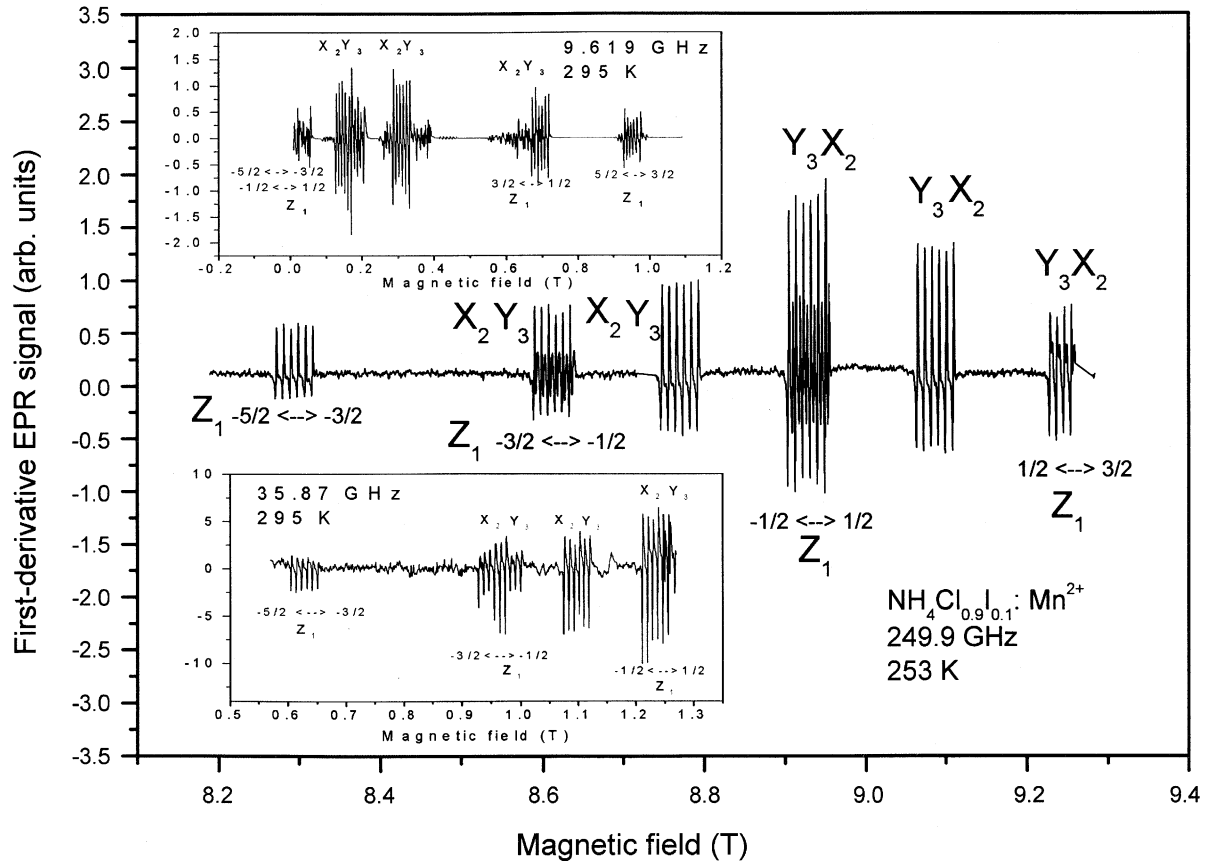
Fig. 2. Observed EPR spectra of the Mn^{2+} ions in the $NH_4Cl_{0.9}I_{0.1}$ single crystal at 249.9 GHz (253 K) for $B||Z_1||X_2||Y_3$ axes. (The subscripts refer to the three magnetically inequivalent ions.) The clearly resolved lines belonging to the three magnetically inequivalent ions are indicated by Z_1, X_2, Y_3 for $B||Z_1$ at 249.9 GHz. The fine-structure transitions corresponding to hyperfine sextets are indicated. The expected lines above 9.3 T are not observed at 249.9 GHz because 9.3 T is the upper limit of the magnetic field available at this frequency. It is seen that the FIR spectrum at 249.9 GHz provides considerable simplification of the spectrum allowing one to easily distinguish the EPR lines belonging to the three magnetically inequivalent ions. The insets show corresponding EPR spectra at X (9.619 GHz, 295 K) and Q (35.87 GHz, 295 K) bands.

$$\mathcal{H} = \mu_B g[B_z S_z + B_x S_x + B_y S_y] + (1/3)b_2^0 O_2^0$$
$$+ (1/60)b_4^0 O_4^0 + A(S_z I_z + S_x I_x + S_y I_y)$$
$$+ Q'[I_z^2 - I(I+1)/3], \qquad (3.1)$$

where the spin operators $O_2^0 = [S_z^2 - S(S+1)/3]$, $O_4^0 = [35S_z^4 - \{30S(S+1) - 25\}S_z^2 + 3S^2 (S+1)^2 - 6S(S+1)]$. In (3.1), $S = 5/2$ is the electronic spin of the Mn^{2+} ion with S_z the Z component of the electronic spin operator, and $I = 5/2$ is the nuclear spin of the ^{55}Mn nucleus; $b_2^0(= D)$ and b_4^0 are the ZFS parameters; Q' is the axial component of the nuclear quadrupole splitting tensor, and μ_B is the Bohr magneton. The $\tilde{g}$ and the HF-structure tensor, $\tilde{A}$, were here assumed to be isotropic consistent with the S-state nature of the Mn^{2+} ion.

The SHP were estimated as follows. First, the fine-structure (FS) parameters were evaluated separately at each frequency band using the least-squares\matrix diagonalization (LSFMD) procedure [24], fitting all the estimated FS EPR line positions, $B_F(M)$, at 9.62, 35.87, and 249.9 GHz at 295, 295, and 253 K, respectively, using Eq. (3.2) below. (Here M, $m = \pm1/2, \pm3/2, \pm5/2$

are the electronic and nuclear magnetic quantum numbers, respectively). The $B_F(M)$ were estimated from, B_{HF} (M, m), the hyperfine (HF) line positions, using the following relation [25]:

$$B_F(M) = (3/4)[B_{HF}(M, 5/2) + B_{HF}(M, -5/2)] - (1/8)$$
$$\times \{[B_{HF}(M, 3/2) + B_{HF}(M, -3/2)]$$
$$+ [B_{HF}(M, 1/2) + B_{HF}(M, -1/2)]\}. \qquad (3.2)$$

The angular variations of the Mn^{2+} FS line positions as well as the line positions calculated using the SH parameters listed in Table 1, obtained at 249.9 GHz, are shown in Fig. 4, which also includes those at 9.6 and 35.9 GHz as insets. The LSFMD procedure was then used to estimate the Mn^{2+} SH parameters by fitting simultaneously all the HF lines observed at X-, Q-, and FIR bands at 295, 295, and 253 K, respectively, assuming that there occurs no significant change in the SHP between 295 and 253 K. They are listed in Table 1. The absolute sign of the parameter b_2^0 could not be determined from the present measurements due to lack of liquid-helium data. The minus sign has been used in accordance with that
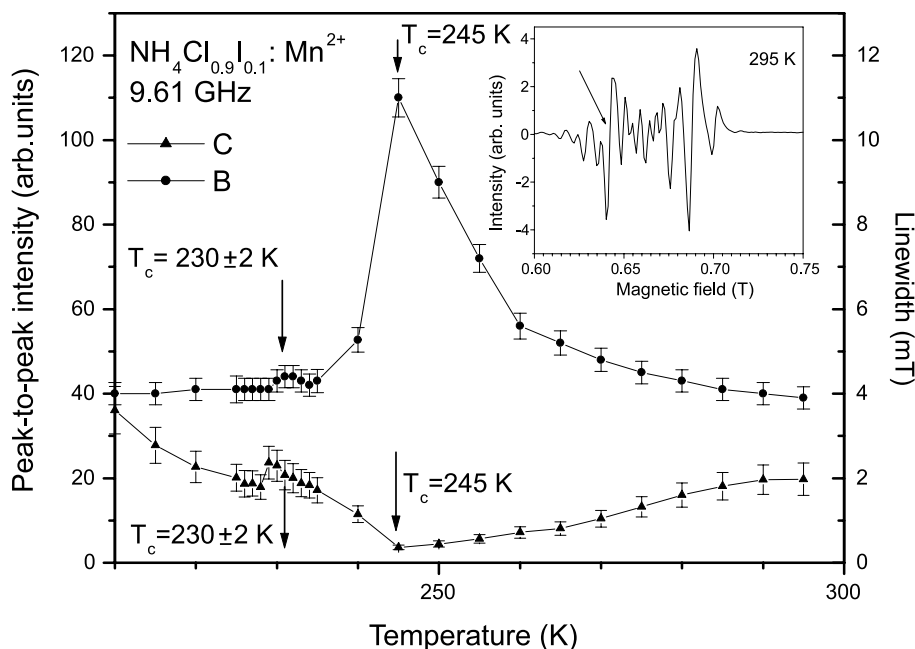
Fig. 3. Temperature variation of the first derivative peak-to-peak height and width of the hyperfine EPR lines belonging to the highest-field sextet at the orientation of B at 60° from the Z-axis in the (0 0 1) plane at 9.6 GHz. The solid circles indicate the observed values for the linewidth, while the triangles indicate the observed peak-to-peak height. An EPR spectrum at room temperature is also shown in the inset, with the arrow indicating the line used for the demonstration of occurrence of phase transition. The continuous lines connect data points as an aid to the eye.

Table 1
Estimated values of the Mn^{2+} spin-Hamiltonian parameters in $NH_4Cl_{0.9}I_{0.1}$ single crystal for one of the magnetically inequivalent ions

	X-band		Q-band		FIR-band	(X + Q + FIR)
	9.619 GHz	9.696 GHz	35.87 GHz	36.06 GHz	249.9 GHz	bands simultaneous fit
Temperature	295 K	125 K	295 K	77 K	253 K	295 K (253 K)
n	180	222	138	276	224	542
g	2.0052 ± 0.0002	1.9986 ± 0.0002	2.0103 ± 0.0001	2.0115 ± 0.0001	1.9997 ± 0.0001	1.9997 ± 0.0001
b_2^0 (GHz)	-4.540 ± 0.001	-4.637 ± 0.001	-4.572 ± 0.001	-4.780 ± 0.001	-4.538 ± 0.001	-4.563 ± 0.001
b_4^0 (GHz)	0.014 ± 0.001	0.001 ± 0.001	0.014 ± 0.001	0.010 ± 0.001	0.009 ± 0.001	0.019 ± 0.001
A (GHZ)	-0.2438 ± 0.0002	-0.2376 ± 0.0002	-0.2547 ± 0.0003	-0.2515 ± 0.0003	-0.2489 ± 0.0003	-0.2502 ± 0.0003
RMSL (GHz)	0.03	0.05	0.05	0.03	0.11	0.11

Due to their physical equivalence, the same SHP values are expected for the other two magnetically inequivalent Mn^{2+} ions. Here n is the number of hyperfine line positions fitted simultaneously in the least-squares procedure; $SMD(GHz^2) = \sum_i(\Delta E_i - v_i)^2$, where ΔE_i is the calculated energy difference in GHz between the levels participating in resonance for the ith line position; v_i is the corresponding klystron frequency in GHz; h is Planck's constant; and $RMSL = (SMD/n)^{1/2}$. The value of Q' was indeterminate within experimental error, and is therefore not listed here.

determined in [4] from the relative intensity of the Mn^{2+} EPR lines at 1.43 K in the NH_4Cl crystal. Since the LSFMD procedure yields the correct relative sign of all the parameters, the signs in Table 1 can then be considered as absolute. The absolute sign of the hyperfine interaction constant A has been determined to be negative from hyperfine-interaction data [26].

4. Application of the superposition model: immediate environment of the Mn^{2+} ion

The spin-Hamiltonian parameters for the Mn^{2+} ion in the mixed single crystal $NH_4Cl_{0.9}I_{0.1}$ can be interpreted in the context of the superposition model (SM)

[27] to better understand the immediate environment of the Mn^{2+} ion. In the superposition model the SHP are expressed as sums of contributions due to the nearest-neighbor ligand ions. When a monovalent (NH_4^+) cation with the ionic radius of 1.43 Å [28] is replaced by a divalent Mn^{2+} cation with the ionic radius of 0.80 Å, charge-compensation occurs to preserve electrical neutrality resulting in the creation of a vacancy near the Mn^{2+} ion, associated with local distortions due to the difference in the impurity and host ion radii [4–6,12–15]. The $NH_4Cl_{0.9}I_{0.1}$ crystal is assumed to have the SC structure, the same as that of NH_4Cl, taking into account the predominantly large proportion (90%) of Cl^- ions. In the $NH_4Cl_{0.9}I_{0.1}$ crystal, on average, 9 out of 10 anions lattice sites will be occupied by the Cl^- ion, while
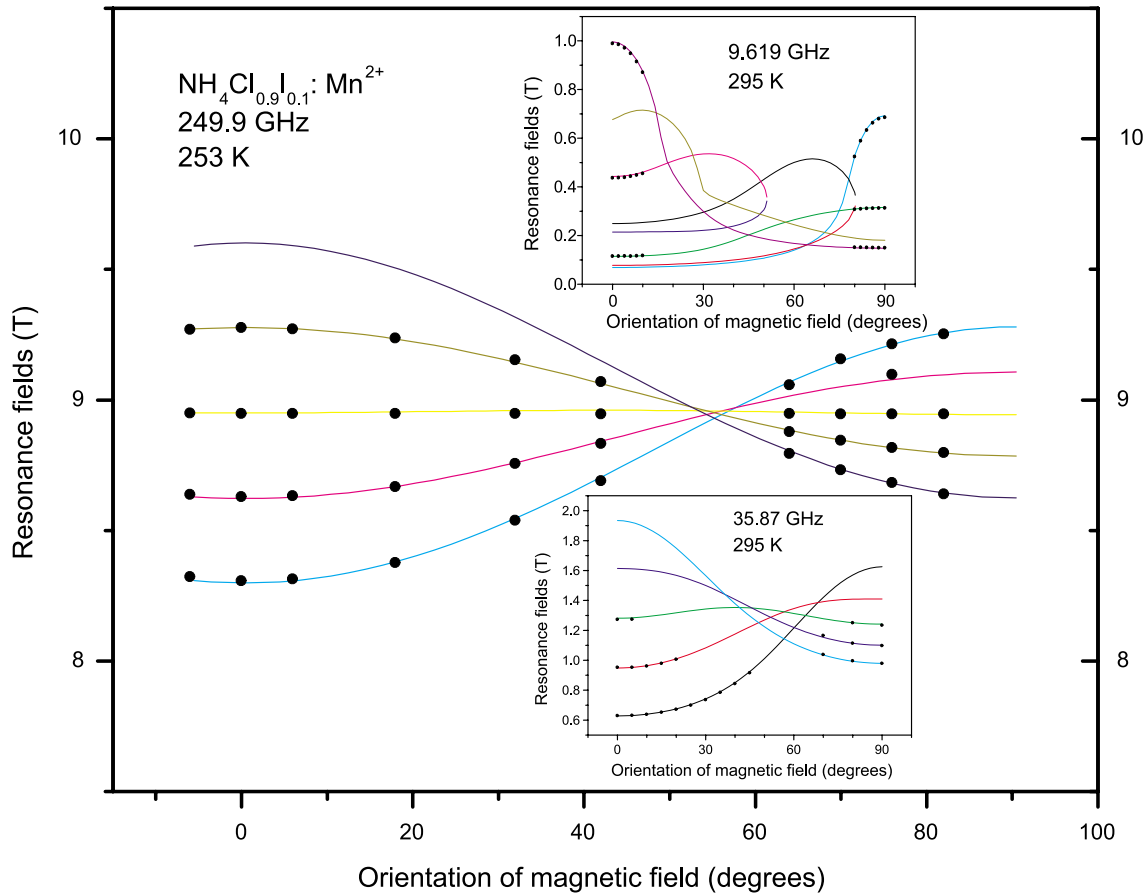
Fig. 4. Angular variation of the fine-structure EPR line positions for one of the three magnetically inequivalent Mn^{2+} ions in $NH_4Cl_{0.9}I_{0.1}$ single crystal at 249.9 GHz at 253 K as deduced from the experimentally observed hyperfine line positions using Eq. (3.2), and those calculated using the SHP listed in Table 1. Solid circles show experimentally observed line positions, while continuous lines show calculated ones. It is noted that due to upper limit on the magnetic field available at 249.9 GHz, EPR lines for $B > 9.3$ T were not observed. The insets show corresponding angular variations at X (9.619 GHz, 295 K) and Q (35.87 GHz, 295 K) bands. The expected EPR lines at Q band for $B > 1.3$ T are also not observed due to the upper limit on the available magnetic field value in the spectrometer.

the remaining one is occupied by the I^- ion for uniform doping.

For the axial symmetry case indicated here by the EPR spectra for each magnetically inequivalent Mn^{2+} ion only the parameters b_2^0 and b_4^0 are non-zero. These can be expressed, within the framework of the superposition model, as sums of the contributions from the various ligands i [27]:

$$b_2^0 = \sum_i 1/2(3\cos^2\theta_i - 1)\bar{b}_2(R_0)(R_0/R_i)^{t_2}, \qquad (4.1)$$

$$b_4^0 = \sum_i 1/8(35\cos^4\theta_i - 30\cos^2\theta_i + 3)\bar{b}_4(R_0)(R_0/R_i)^{t_4}.$$

$$(4.2)$$

In (4.1), the Mn^{2+} cation is assumed to be at the origin $(0,0,0)$ of a coordinate system located within the crystal, with the ith Cl^-, or I^-, ligand ion located at position (R_i, θ_i, ϕ_i) relative to this cation; here the variable R_i denotes the distance between the impurity cation

and the ith ligand ion. R_0 is the reference ligand distance and t_n is a power law exponent. For the Mn^{2+} ion [27,29], t_2 and t_4 are usually assumed to to be equal: 7 ± 1. For $NH_4Cl_{0.9}I_{0.1}$, $\theta_i = \pm54.74°$ for the eight ligand Cl^- or I^- ions which are situated at the vertices of a cube in the SC structure, with the Mn^{2+} ion situated at its center, and the Z-axis oriented along one of the crystallographic axes [1 0 0], [0 1 0], [0 0 1], as shown in Fig. 1 for this configuration. It is found from Eq. (4.1), since $3\cos^2\theta = 1$ for $\theta = \pm54.74°$, that the parameter $b_2^0 = 0$, when the Mn^{2+} ion replaces an NH_4^+ ion at its crystallographic position and no displacement of any ligand from its original position occurs. In order for this parameter to become large, and for the local site symmetry to become axial, as observed in this work, it is necessary that: (i) the Mn^{2+} ion be displaced sufficiently along a cubic axis from the NH_4^+ position so that θ_i is significantly different from 54.74°, (ii) a redistribution of ligand ions occurs to produce an axially symmetry crystal field at the Mn^{2+} ion, and (iii) the vacancies due

to charge-compensation occur at NH_4^+ sites adjacent to an Mn^{2+} ion on the cubic axis on which the displacement of the Mn^{2+} ion takes place. There are thus six possible positions for these vacancies consistent with the presence of three magnetically inequivalent ions with their respective magnetic Z-axes oriented along the three crystallographic axes, each ion exhibiting an axially symmetric spectrum about its own Z-axis.

To explain the observed axial symmetry of the $NH_4Cl_{0.9}I_{0.1}$ crystal, as opposed to the tetragonal symmetry expected from the undisplaced positions of ligands, it is proposed here that the Mn^{2+} ion, in conjunction with the vacancy, causes a significant reorganization of its immediate environment such that it sees an axially symmetric crystal field at its site. The experimental value of $b_2^0 = -4.56$ GHz estimated here is rather large for an inorganic crystal host [19]. Furthermore, almost the same values, $b_2^0 = -4.515$ and -4.498 GHz, were observed for the Mn^{2+} ion in NH_4I and NH_4Cl with FCC and SC structures, respectively [4,12]. This implies that substitution of a divalent Mn^{2+} ion for a monovalent NH_4^+ ion in both the NH_4Cl and NH_4I crystals, and thus in the mixed $NH_4Cl_{0.9}I_{0.1}$ crystal, results in a significant local rearrangement near the Mn^{2+} ion. These are almost the same for the two cubic structures SC and FCC of the NH_4Cl and NH_4I crystals, respectively. Thus the NH_4^+ ions play the dominant role in determining the spin-Hamiltonian parameters in NH_4I, and NH_4Cl, and the halide ions, Cl^- and I^-, contribute to the Mn^{2+} SHP only in a marginal manner.

5. Discussion and concluding remarks

The salient features of the EPR studies presented here are as follows:

(i) FIR EPR at 249.9 GHz provides a considerable simplification of the EPR spectrum making it quite easy to distinguish the three magnetically inequivalent Mn^{2+} ions, which is rather difficult at X (9.6 GHz) and Q (36 GHz) bands.

(ii) The symmetry of Mn^{2+} EPR spectra and the values of the SH parameters indicate that the Mn^{2+} ions are displaced from the NH_4^+ positions along the three cubic axes accompanied by a vacancy at adjacent NH_4^+ sites in the direction of the displacement for charge-compensation. As a consequence, the immediate environment around an Mn^{2+} ion in the $NH_4Cl_{0.9}I_{0.1}$ cubic crystal is changed considerably from that at an NH_4^+ site, so that an axially symmetric crystal field is produced at its site. The same is true of the Mn^{2+}-doped NH_4I and NH_4Cl crystals [4–6,12–15]. As a consequence all the crystals, NH_4Cl, NH_4I, and $NH_4Cl_{0.9}I_{0.1}$ are characterized by about the same values of the parameters b_2^0 and b_4^0 for the Mn^{2+} ion, with axial symmetry about its Z-axis.

(iii) Vacancies are created due to charge-compensation resulting from substitution of divalent Mn^{2+} ions for monovalent NH_4^+ ions. These are situated at the next-neighbor sites to Mn^{2+} ions in the [1 0 0], [0 1 0], [0 0 1] crystallographic directions. This results in three magnetically inequivalent, but physically equivalent, Mn^{2+} ions in the mixed $NH_4Cl_{0.9}I_{0.1}$ single crystal with the three magnetic Z-axes oriented along the cube edges.

(iv) Very accurate values of the SHP have here been estimated by fitting simultaneously all EPR line positions observed at X-, Q-, and FIR bands.

(v) The temperature variation of the Mn^{2+} EPR linewidth and peak-to-peak intensity of some of the highest-field lines in the range 120–300 K clearly indicate occurrence of λ-phase transitions at 245 and 230 K, corresponding to transitions observed in the pure NH_4Cl and NH_4I crystals.

References

[1] A.G. Brenosa, F. Rodriguez, M. Moreno, Ferroelectrics 106 (1990) 187.
[2] H. Abe, H. Shirai, J. Phys. Soc. Jpn. 15 (1960) 1711.
[3] M.M. Zaripov, G.K. Chirkin, Z. Struct. Khim. 5 (1964) 36.
[4] M.M. Zaripov, G.K. Chirkin, Sov. Phys. Solid State 7 (1966) 2391.
[5] A. Forman, J.A. van Wyk, J. Chem. Phys. 44 (1966) 73.
[6] A. Forman, J.A. van Wyk, Can. J. Phys. 45 (1967) 3381.
[7] T.J. Seed, J. Chem. Phys. 41 (1964) 1486.
[8] V. Lupei, A. Lupei, F. Domsa, J. Magn. Reson. 19 (1975) 337.
[9] R. Bramley, S.J. Strach, Chem. Phys. Lett. 79 (1981) 183.
[10] J.A. Kennewell, J.R. Pilbrow, J.H. Price, Phys. Lett. A 27 (1968) 228.
[11] J.A. Van Wyk, J. Magn. Reson. 18 (1975) 235.
[12] P. Chand, G.C. Upreti, J. Chem. Phys. 78 (1983) 5930.
[13] P. Chand, G.C. Upreti, J. Chem. Phys. 81 (1984) 1650.
[14] P. Chand, G.C. Upreti, S.K. Misra, M. Bartkowski, J. Chem. Phys. 82 (1985) 5307.
[15] P. Chand, Ph.D. thesis. Electron paramagnetic resonance study of ammonium iodide single crystals doped with Cu^{2+}, Mn^{2+}, and VO^{2+} submitted to Indian Institute of Technology (IIT), Kanpur, India, 1983 and the references cited in the thesis in this context.
[16] S.K. Misra, in: C.P. Poole Jr., H.A. Farach (Eds.), Handbook of Electron Spin Resonance, vol. 2, Springer, New York, 1999, p. 85.
[17] M.D. Sastry, Ph.D. thesis, I.I.T. Kanpur, India, 1967.
[18] S.K. Misra, S.I. Andronenko, K.A. Earle, J.H. Freed, Appl. Magn. Reson. 21 (2001) 549.
[19] S.K. Misra, in: A. Kawamori, Y. Yamauchi, H. Ohta (Eds.), High-Frequency Single-Crystal EPR Application to Multifrequency Approach: Study of Metalloproteins, EPR in the 21st

Century, Elsvier Science, Amsterdam, 2002, pp. 731–740, Refereed Proceedings of the Asia Pacific EPR Society, 2001 conference, Kobe, Japan.

[20] L. Vegard, Z. Phys. 5 (1921) 17.

[21] H.A. Levy, S.W. Peterson, J. Am. Chem. Soc. 75 (1953) 1536.

[22] W.B. Lynch, K.A. Earle, J.H. Freed, Rev. Sci. Instrum. 59 (1988) 1345.

[23] S.K. Misra, J. Sun, Magn. Reson. Rev. 16 (1991) 157.

[24] S.K. Misra, J. Magn. Reson. 23 (1976) 406.

[25] S.K. Misra, Physica B 121 (1983) 193.

[26] A. Steudel, in: Hyperfine Interaction, Academic Press, New York, 1976, p. 182.

[27] D.J. Newman, Adv. Phys. 20 (1971) 197.

[28] C. Kittel, Introduction to Solid State Physics, Wiley, New York, 1961.

[29] D.J. Newman, W. Urban, Adv. Phys. 24 (1975) 793.